

An Arecibo follow-up study of seven pulsars discovered by Five-hundred-meter Aperture Spherical radio Telescope (FAST)

Shen Wang (王坤)^{1,2}, Wei-Wei Zhu (朱炜玮)¹, Di Li (李葭)^{*1,2,3}, Zhi-Chen Pan (潘之辰)¹, Pei Wang (王培)¹, James M. Cordes^{4,5}, Shami Chatterjee^{4,5}, Ju-Mei Yao (姚菊枚)^{1,6}, Lei Qian (钱磊)¹, You-Ling Yue (岳友岭)¹, Lei Zhang (张蕾)¹, Ru-Shuang Zhao (赵汝双)^{1,7}, Shuang-Qiang Wang (王双强)⁶, Jia-Rui Niu (牛佳瑞)^{1,2}, Mao Yuan (袁懋)^{1,2}, Chen-Chen Miao (缪晨晨)^{1,2}, Xiao-Yao Xie (谢晓尧)⁷, Zhi-Jie Liu (刘志杰)⁷, Xu-Hong Yu (于徐红)⁷, Shan-Ping You (游善平)⁷, Ling-Qi Meng (孟令祺)^{1,2} and FAST Collaboration¹

¹ National Astronomical Observatories, Chinese Academy of Sciences, 20A Datun Road, Chaoyang District, Beijing 100101, China; dili@nao.cas.cn; zhuww@nao.cas.cn

² College of Astronomy and Space Sciences, University of Chinese Academy of Sciences, Beijing 100049, China

³ NAOC-UKZN Computational Astrophysics Centre, University of KwaZulu-Natal, Durban 4000, South Africa

⁴ Department of Astronomy, Cornell University, Ithaca, NY 14853, USA

⁵ Cornell Center for Astrophysics and Planetary Science, Cornell University, Ithaca, NY 14853, USA

⁶ Xinjiang Astronomical Observatories, Chinese Academy of Sciences, 150, Science 1-Street, Urumqi 830011, China

⁷ Guizhou Normal University, Guiyang 550001, China

Received 2021 March 16; accepted 2021 June 28

Abstract We present Arecibo 327 MHz confirmation and follow-up studies of seven new pulsars discovered by the Five-hundred-meter Aperture Spherical radio Telescope (FAST). These pulsars are discovered in a pilot program of the Commensal Radio Astronomy FAST Survey (CRAFTS) with the ultra-wide-bandwidth commissioning receiver. Five of them are normal pulsars and two are extreme nulling slow pulsars. PSR J2111+2132's dispersion measure ($DM: 78.5 \text{ pc cm}^{-3}$) is above the upper limits of the two Galactic free electron density models, NE2001 and YMW16, and PSR J2057+2133's position is out of the Scutum-Crux Arm, making them uniquely useful for improving the Galactic free electron density model in their directions. We present a detailed single pulse analysis for the slow nulling pulsars. We show evidence that PSR J2323+1214's main pulse component follows a non-Poisson distribution and marginal evidence for a sub-pulse-drift or recurrent period of 32.3 ± 0.4 rotations from PSR J0539+0013. We discuss the implication of our finding to the pulsar radiation mechanism.

Key words: methods: observational, pulsars: general, stars: neutron

1 INTRODUCTION

Pulsars are stellar remnants with densities higher than the atomic nucleus. They produce radio beams that sweep across the sky like lighthouses. Pulsars can be used to study the interstellar medium, neutron star physics, planetary physics, celestial mechanics and cosmology (Lorimer et al. 2006). The number of known pulsars has increased steadily to over 3000 (Han et al. 2021) in the past five decades since the first discovery in 1967 (Hewish et al. 1968).

The Commensal Radio Astronomy FAST Survey (CRAFTS) is designed to be carried out in drift-scan mode and to observe HI and pulsars simultaneously for

optimum efficiency (Nan et al. 2011; Li et al. 2018, 2019). Enabled by a novel high-cadence CAL injection technique, CRAFTS simultaneously records pulsar-search, HI-galaxy, HI-imaging and radio-transient data streams, relying on multiple backends (Li et al. 2018). We tested this survey mode in 2017 during the commissioning and early science phases of Five-hundred-meter Aperture Spherical radio Telescope (FAST), with the ultra-wide-band (UWB) receiver covering 270 to 1620 MHz. CRAFTS discovered its first pulsar (Qian et al. 2019) in the commission phase. In 2018, the UWB was replaced with the FAST L-band Array of 19-beams (FLAN: Li et al. 2018). By now, CRAFTS has discovered more than

120 confirmed new pulsars¹, including 16 slow pulsars ($P \geq 2$ s), by utilizing the UWB and the FLAN.

This paper presents the Arecibo confirmation study of seven CRAFTS-discovered pulsars, including five normal pulsars and two slow ones. The periods, dispersion measures (DMs) and positions of six of the pulsars are published for the first time. The slow pulsar PSR J2323+1214 was timed at the Parkes telescope and its precisely measured position and timing parameters were reported in Cameron et al. (2020). The two slow pulsars presented in this paper exhibit interesting single pulse variations. Such phenomenon is best studied employing a large telescope in low observing frequency bands where the pulsars are relatively bright. Therefore, we devote a substantial portion of this paper to the single pulse study of these two slow pulsars: PSR J2323+1214 (3.76 s) and PSR J0539+0013 (4.71 s). Our result indicates that these two slow pulsars might be members of the extremely nulling pulsars and studies of their single pulse behavior may help us understand the emission mechanism of pulsars.

The pulsar nulling phenomenon was first discovered by Backer (1970). For some pulsars, the nulls are one to three pulses long, and for others, the nulls could last for many rotations and sometimes hours. Ruderman & Sutherland (1975) established the canonical model for the pulsar emission mechanism, which also offers an explanation for the nulling phenomenon. They suggested that the nulling phenomenon happens when the pair plasma generated from the vacuum gap shorts the gap. Wang et al. (2007) and Lyne et al. (2010) suggested that nulling is related to mode changing and a manifestation of change in a pulsar’s magnetospheric current flows. Filippenko & Radhakrishnan (1982) argued that nulling is a continuous and steady discharge in the polar gap rather than a complete cessation of sparking.

Hitherto, over 140 nulling pulsars have been identified (Sheikh & MacDonald 2021) and 29 of them manifest periodic nulling (Basu et al. 2020b). In many cases the switching between the burst and the null is considered to be a stochastic process (Ritchings 1976; Biggs 1992; Basu et al. 2017), while in some other cases the transition from the null to the burst states has shown periodicity (Herfindal & Rankin 2007, 2009). Herfindal & Rankin (2007) first discovered the periodic nulling phenomenon (from PSR B1133+16), which implies an additional physical process in the emission of nulling pulsars. They suggest that this phenomenon may be related to the periodic modulation of the pulse profile.

¹ The confirmed new pulsar list can be found at <https://crafts.bao.ac.cn/pulsar/>.

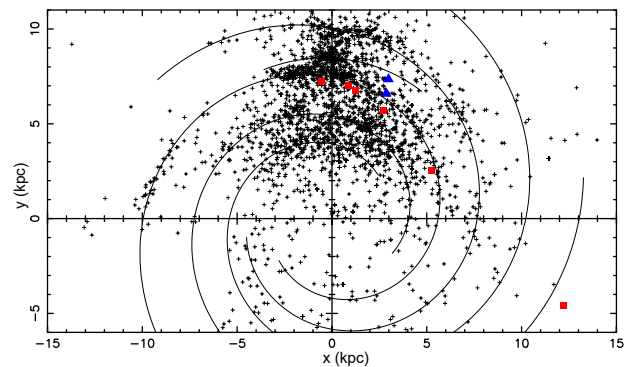


Fig. 1 A pulsar location diagram displaying the six discovered pulsars (red squares) against the known pulsar population and two unconfirmed pulsar candidates (blue triangles) on the Milky Way. PSR J2111+2132 is not described well by the two Galactic free electron density models, NE2001 and YMW16, and thus not displayed in the figure.

In this work, we describe seven pulsars discovered by FAST UWB and confirmed by Arecibo. We describe the FAST search observation, the Arecibo confirmation observation and single pulse analysis in Section 2. We report the results of confirmation and data analysis in Section 3. A summary is given in Section 4.

2 OBSERVATIONS AND DATA REDUCTION

2.1 FAST and CRAFTS Survey

FAST has become the largest and most sensitive single-dish radio telescope since the initiation of its formal operation on 2020 January 11 (Nan et al. 2011; Jiang et al. 2019). The CRAFTS program started with an ultra-wide-bandwidth receiver and later switched to FLAN. All pulsars reported here were discovered in frequency bands lower than 1 GHz and hereafter referred to as CRAFTS-UWB sources. CRAFTS-UWB has 8192 channels over the full band with a channel bandwidth of 0.25 MHz. The typical system temperatures are $T_{\text{sys}} = 60\text{--}70$ K since the UWB was not cryogenic. The CRAFTS-UWB survey utilized drift-scan mode, corresponding to an integration time of only 12–50 s per beam, depending on the frequency (Li et al. 2018). For example, the UWB beam’s full width at half maximum (FWHM) is about 15’ for 270 MHz, corresponding to a source crossing time of one minute at $\delta = 0^\circ$.

The CRAFTS-UWB pilot survey was processed through multiple pipelines, including periodicity searches (Yu et al. 2020) and single pulse searches aided by deep learning (Zhu et al. 2014). The CRAFTS-UWB has discovered 53 confirmed pulsars in total, among them seven were confirmed by Arecibo (this work and one

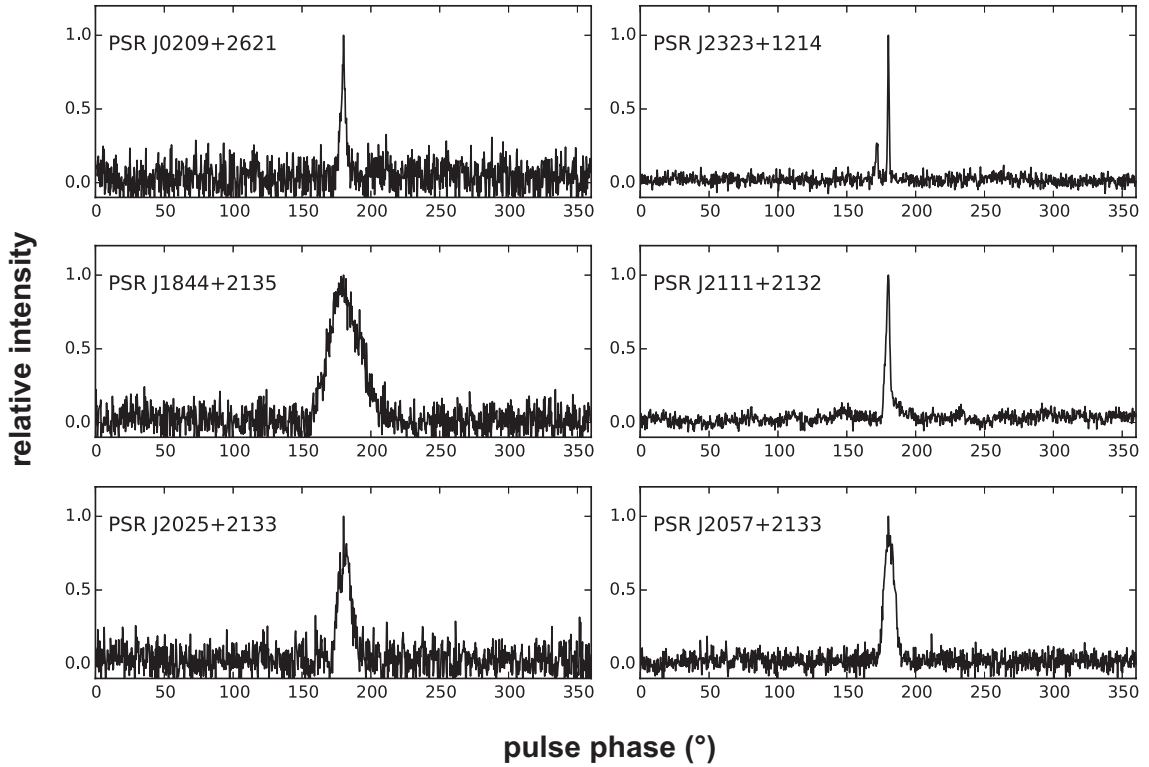


Fig. 2 The pulse shapes of the confirmed pulsars, except PSR J0539+0013.

also in Cameron et al. 2020), 14 were confirmed by Parkes (11 published in Cameron et al. 2020 and three unpublished), 10 were confirmed by Effelsberg (Cruces et al. submitted) and 23 were confirmed by FAST itself in the later CRAFTS-FLAN survey (Wang et al. in prep); 49 out of the 53 confirmed pulsars have DM less than 150 pc cm^{-3} (about 92%); 21 out of 53 (40%) have periods longer than 1.5 s.

2.2 Arecibo Observations

Arecibo was the only telescope in the world with sensitivity matching FAST in the 300 MHz band and was ideal for confirming FAST candidates. We proposed to Arecibo and got 20 hours to follow up FAST candidates (P3270). Because PSR J0539+0013’s initial position is less constrained than those of other candidates, we tried to grid search PSR J0539+0013 with four pointings in the Arecibo observation. We observed each point for 10 minutes and successfully detected the pulsar in one of the positions, thus constraining its position to a precision of $15'$. We performed confirmation observations for the other eight candidates and observed each one for about 45 to 60 minutes. In summary, we confirmed seven pulsars: PSRs J0209+2621, J2323+1214, J1844+2135, J0539+0013, J2111+2132, J2025+2133 and J2057+2133, but failed to detect two

candidates J1914+2624 and J2223+0818, probably due to uncertainty in the candidate positions.

For the confirmation observations, we used the Puerto Rico Ultimate Pulsar Processing Instrument (PUPPI) backend with 100 MHz of bandwidth split into 4096 channels sampled at $82 \mu\text{s}$ (“fast4k” mode). The effective bandwidth is 68.75 MHz (2816 channels), a standard mode in CIMA. The data were recorded with 8-bit sampling using PSRFITS format (Hotan et al. 2004) without polarization.

The observation information is listed in Table 1. The candidate J2323+1214 has been confirmed by both Arecibo and Parkes. The confirmation results from Arecibo are displayed in Table 2 and Figure 2. Details on each pulsar’s parameters are reported in Section 3.

2.3 Data Reduction and Single Pulse Analysis

We perform and search the best fit period and DM of each candidate with PSRCHIVE² software package (Hotan et al. 2004). We fold the pulsar candidates with their best fit period and DM employing the digital signal processing of pulsar time-series (DPSR³) software package (van Straten & Bailes 2010). Five (PSRs J0209+2621, J1844+2135, J2111+2132,

² <http://psrchive.sourceforge.net/index.shtml>

³ <https://github.com/demorest/dpsr>

Table 1 The Summary of Arecibo Confirmation Observation (P3270)

PSR Name	Date (AST)	RA ^a (J2000)	Dec ^a (J2000)	T _{obs} (min)	Detection (Y/N)
J0539+0013	2018-9-19	05:38:55	+00:13:36	10	N
		05:39:20	+00:13:36	10	N
		05:39:45	+00:13:36	10	Y
		05:40:10	+00:13:36	10	N
J0209+2621	2018-9-27	02:09:00	+26:21:22	60	Y
J1844+2135	2018-9-28	18:44:56	+21:35:55	45	Y
J1914+2624	2018-9-28	19:14:52	+26:24:01	45	N
J2025+2133	2018-10-1	20:25:40	+21:33:39	60	Y
J2057+2133	2018-10-1	20:57:40	+21:33:03	60	Y
J2111+2132	2018-10-1	21:11:45	+21:32:41	51	Y
J2223+0818	2018-10-1	22:23:35	+08:18:30	26	N
J0539+0013	2018-11-27	05:39:45	+00:13:36	40	Y
J2323+1214	2019-4-19	23:23:21	+12:08:35	100	Y

a. The positions presented here are the best guesses for the confirmation observation by Arecibo.

Table 2 The Confirmation Results of FAST Pulsar Candidates

PSR Name	RA (J2000)	Dec (J2000)	P (ms)	DM (pc cm ⁻³)	NE2001 (pc)	YMW16 (pc)
J0209+2621	02:09(1)	+26:21(15)	1934.8	23.7	1022	1732
J2323+1214	23:23(1)	+12:14(15)	3759.5	26.7	1448	3852
J1844+2135	18:44(1)	+21:35(15)	594.6	29.2	1993	1599
J0539+0013	05:39(1)	+00:13(15)	4710.2	49.0	2044	1399
J2111+2132	21:11(1)	+21:32(15)	1059.5	78.5	>50 000	>25 000
J2025+2133	20:25(1)	+21:33(15)	623.5	70.8	3850	5942
J2057+2133	20:57(1)	+21:33(15)	1166.7	72.2	4603	13809

J2025+2133 and J2057+2133) are normal pulsars. Two of them (PSRs J2111+2132 and J0539+0013), the slowest of the seven, are nulling pulsars with significant pulse-to-pulse variations.

We follow the previous studies of nulling pulsars (Ruderman & Sutherland 1975; Ritchings 1976; Biggs 1992; Herfindal & Rankin 2007; Wang et al. 2007; Herfindal & Rankin 2009; Redman & Rankin 2009; Gajjar et al. 2012; Cordes 2013; Gajjar et al. 2014; Basu et al. 2017, 2020b). We plot the energy distributions of two slow pulsars to identify them as nulling pulsars and further confirm them as extreme nulling pulsars because of their high nulling fractions (>75%). We employ two different methods, the *runs* test and the waiting time analysis to test the statistical behavior of the single-pulse sequences, specifically, whether the single pulses follow a Poisson process in which the occurrence of a pulse does not depend on its previous pulse (Redman & Rankin 2009; Cordes 2013; Basu et al. 2017). A Poisson pulse distribution favors that the pulses were simply varying in brightness and not really shutting off in between bursts, while a non-Poisson distribution may suggest the presence of intermittent sparks as suggested in some models (Ruderman & Sutherland 1975; Gil et al. 2003; Szary et al. 2015). We also adopt a periodogram-based arrival time analysis to search for a potential recurrent

period or quasi-periods in a timescale longer than most of the pulse-to-pulse waiting times.

Energy Distribution Study: Nulling behavior is usually identified through a bimodal distribution in the single-pulse energy distribution of the pulsar (Basu et al. 2017). We follow the analysis described in Weltevrede et al. (2006) and rely on the software PSRSALSA package (Weltevrede 2016) to plot the energy distributions of the two slow pulsars. We fit the pulses of the main and secondary components of PSR J2323+1214 separately. Because PSR J0539+0013’s two components are connected by a bright emission, here we treat it as one component. We then chose the same number of phase bins in the on-phase and off-pulse regions, and the PSRSALSA package to compute the integral difference between the on-pulse and the off-pulse. The result reflects the energy of the single pulse (E) in an arbitrary unit. We could see clear bimodal distributions in E as depicted in Figure 4 and Figure 7.

Nulling Fraction Analysis: The nulling fraction describes the time fraction of the pulsar nulling. Ritchings (1976) finds that nulling fraction is related to the age of pulsars. Biggs (1992) concluded that it is also related to the period. Wang et al. (2007) confirm that nulling fraction is positively correlated with pulsar period and age on the P - \dot{P} diagram. Slow, old pulsars with low rotational energy

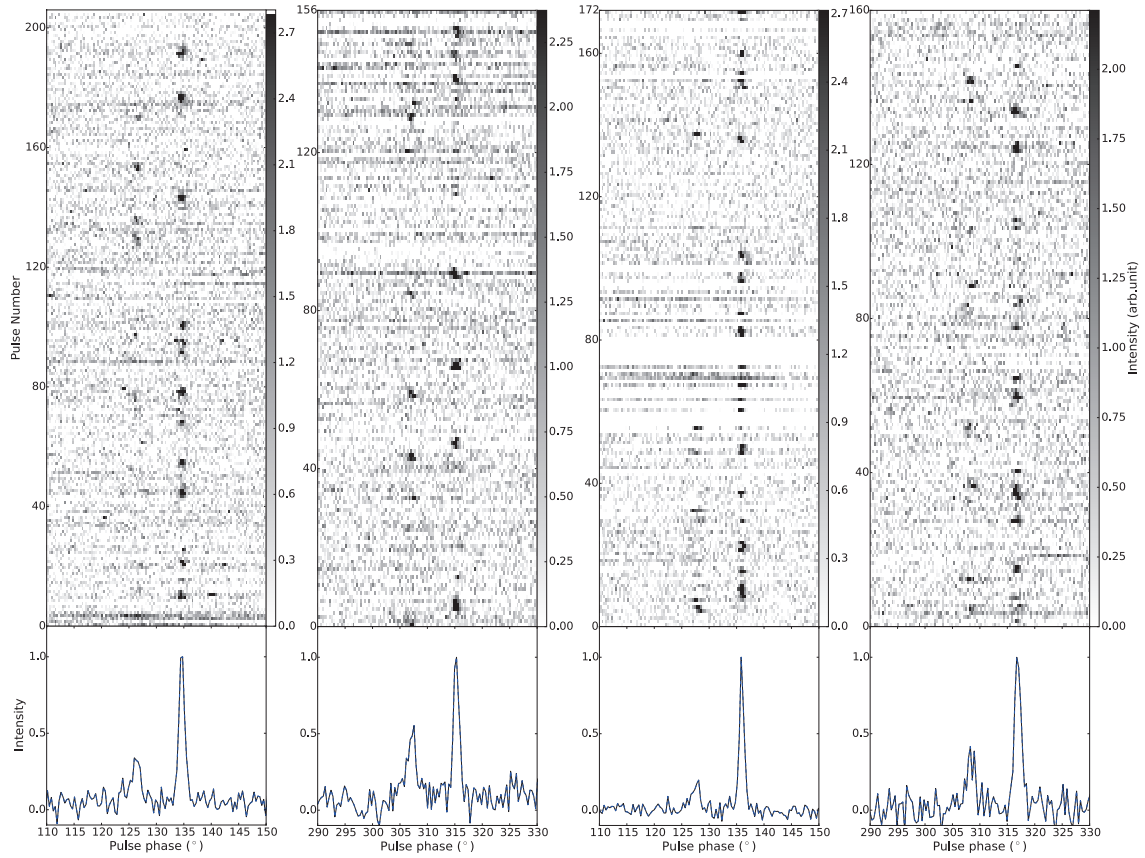


Fig. 3 The pulse stack of PSR J2323+1214.

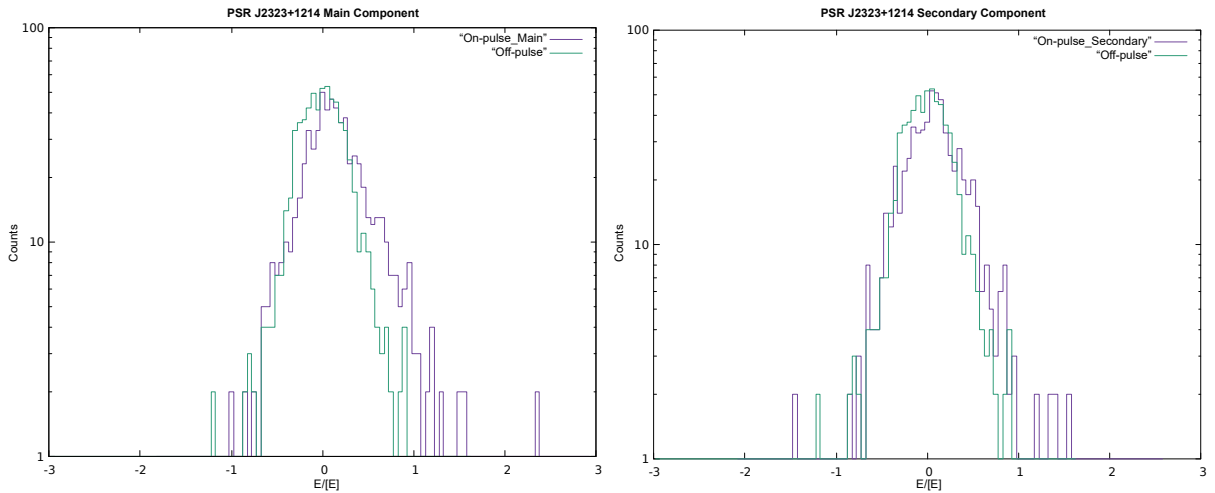


Fig. 4 The on-pulse energy and off-pulse histograms of the main and secondary components of PSR J2323+1214 by PSRSALSA. Because of the high nulling fraction and low flux, the difference between on-pulse and off-pulse for the secondary component is not as clear as the main component.

loss rate \dot{E} tend to be more likely to null. Conventionally, a pulsar with nulling fraction greater than 75% is considered an extreme nulling pulsar (Naidu et al. 2018) and there were a total of eight known extreme nulling pulsars (Konar & Deka 2019) before our work.

We plot pulse stacks of slow pulsars PSR J2323+1214 and PSR J0539+0013 in Figure 3 and Figure 8, respectively. Because of the high sensitivity of Arecibo, we could distinguish the nulls and bursts by eye. Through counting the number of pulse-on rotations ($S/N > 3\sigma$)

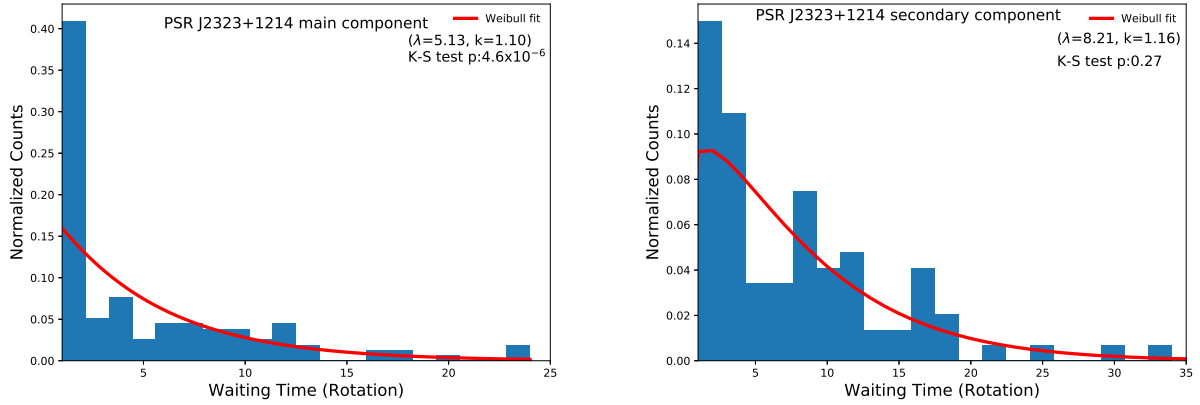


Fig. 5 The waiting time histogram of the two components of PSR J2323+1214.

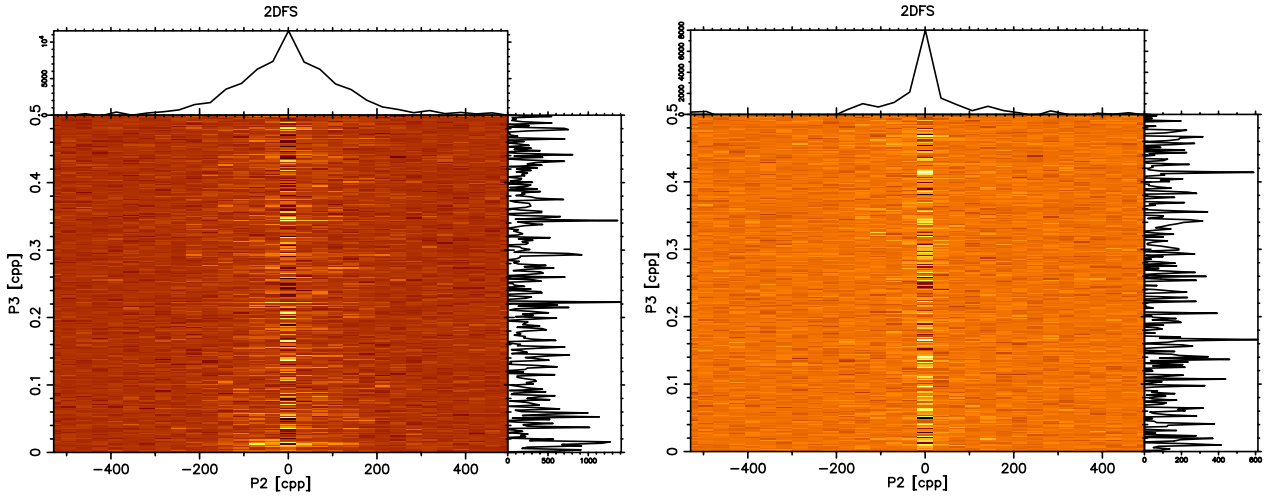


Fig. 6 The subpulse modulation and fluctuation analysis results of PSR J2323+1214 by PSRSALSA. Both of the components have no credible recurrent periodicity.

and pulse-off rotations, we detect 135 pulses out of 694 rotations for PSR J2323+1214’s main component and 88 pulses out of 694 rotations for its secondary component. We detect 52 pulses out of 328 rotations for PSR J0539+0013. Thus, PSR J2323+1214 has a nulling fraction of $(80\pm 2)\%$ for its main component and $(87\pm 1)\%$ for its secondary component, and PSR J0539+0013 has a nulling fraction of $(84\pm 2)\%$.

Before the periodic nulling phenomenon was discovered, pulsar nulling has generally been assumed to be occurring randomly with equal chances in time. Redman & Rankin (2009) first used a statistic Z based on the *runs* test proposed by Wald & Wolfowitz (1940) to test the distribution of pulsar single pulses. The same method was also utilized in the following works (Cordes 2013; Basu et al. 2017).

We adopt and apply the same *runs* test on our pulsars. If the pulses of a pulsar follow a Poisson distribution with a constant occurrence rate, then the number of observed runs (R), i.e. the number of transitions between the nulls (N_1) and bursts (N_2), follows a normal distribution around μ

$$\mu = \frac{2N_1N_2}{N_1 + N_2} + 1, \quad (1)$$

with a standard deviation σ

$$\sigma = \sqrt{\frac{2N_1N_2(2N_1N_2 - N_1 - N_2)}{(N_1 + N_2)^2(N_1 + N_2 - 1)}}. \quad (2)$$

As a result, the statistic $Z = (R - \mu)/\sigma$ follows a Gaussian distribution with zero mean and unit standard deviation. If $-1.96 < Z < 1.96$, the sequence is indistinguishable from a uniform-rate Poisson process at the 0.05 significance level (Redman & Rankin 2009). Here,

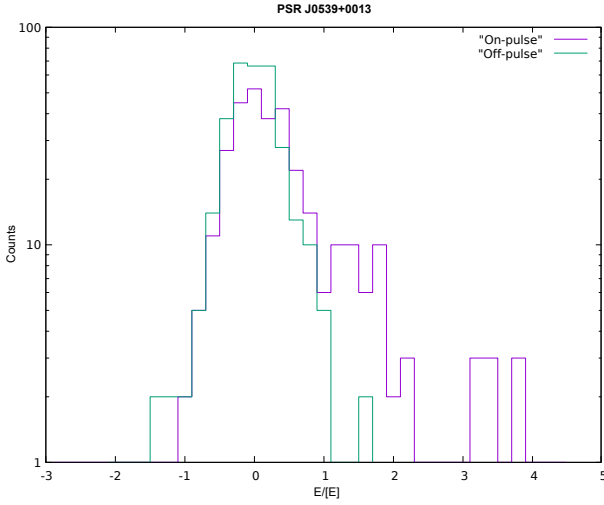


Fig. 7 The on-pulse energy and off-pulse energy histograms of PSR J0539+0013 by PSRSALSA.

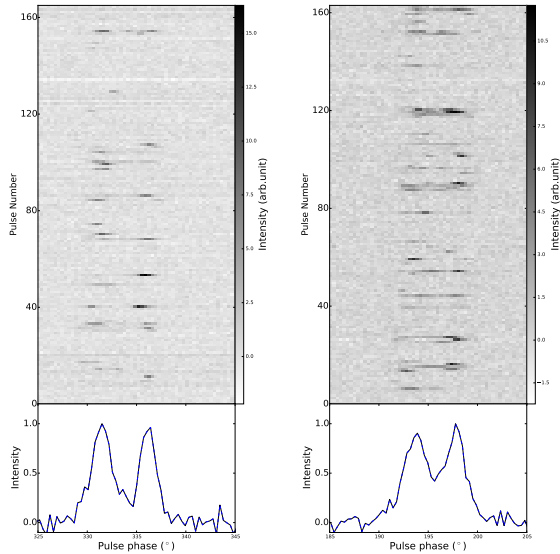


Fig. 8 The pulse stack of PSR J0539+0013.

the statistic of PSR J2323+1214's main and secondary components are $Z = -6.6$, $\sigma = 8.2$ and $Z = -2.2$, $\sigma = 5.8$, respectively. The *runs* test of the single pulses of PSR J2323+1214 shows significant deviation from a constant-rate Poisson distribution, with a bias toward over-clustering. For PSR J0539+0013, the statistic $Z = -0.5$ and $\sigma = 4.8$. Here the Z statistic has a standard deviation of 1. It means the single pulses of PSR J0539+0013 may be following a Poisson-like process, which is also consistent with the waiting time analysis.

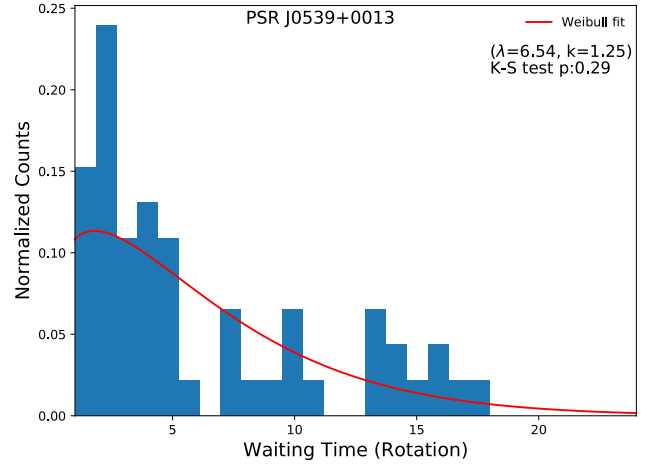


Fig. 9 The waiting time histogram of PSR J0539+0013.

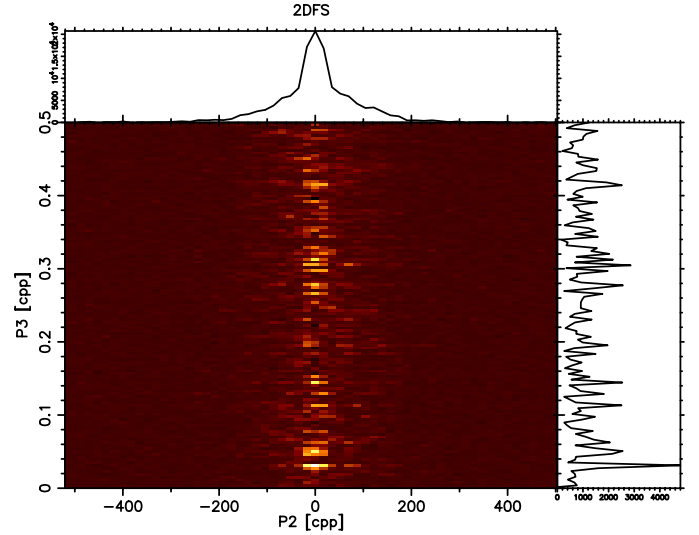


Fig. 10 The subpulse modulation and fluctuation analysis result of PSR J0539+0013 by PSRSALSA. The drifting periodicity (P3) has evidence (signal at 4.4σ level) of a sub-pulse-drift or recurrent period of 32.3 ± 0.4 rotations.

Waiting Time Analysis: As indicated by the aforementioned *runs* test, the single pulses of some pulsars may be over-clustered and deviate from a constant-rate Poisson process (Redman & Rankin 2009; Basu et al. 2017, 2020b). We display the waiting time between pulses in units of rotation for the two components of PSR J2323+1214 (Fig. 5) and the waiting time of PSR J0539+0013 (Fig. 9) and test them against Weibull distributions. This helps us judge whether the pulses come from a Poisson-like process. Here a Weibull distribution (Oppermann et al. 2018) follows

$$f(x; k, \lambda) = \frac{k}{\lambda} \left(\frac{x}{\lambda}\right)^{k-1} e^{-(x/\lambda)^k}, \quad (3)$$

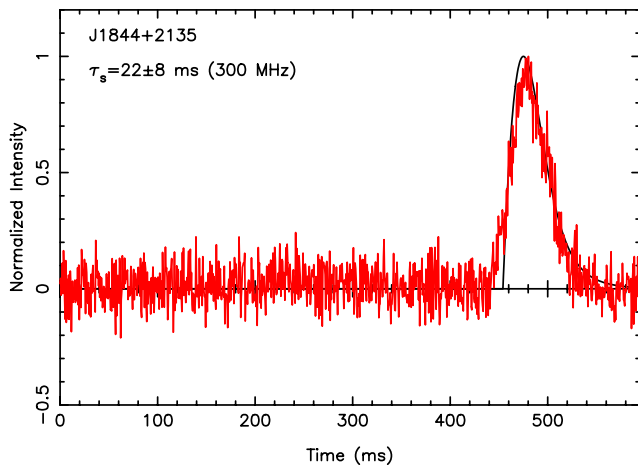


Fig. 11 The pulse profile of PSR J1844+2135 (red line) and the best fit of it (black line).

where x is the waiting time, k is the shape parameter and λ is the scale parameter. A Weibull distribution describes a generalized Poisson process, and it goes back to Poisson when the shape parameter $k=1$. When $k < 1$, the distribution is skewed toward over-clustering, and otherwise over-scattering. We fit the unbinned waiting times (by rotations) of PSR J2323+1214 and PSR J0539+0013 with Weibull distributions. We find the p -values of the Kolmogorov-Smirnov test (K-S test) for the best fit models are 4.6×10^{-6} , 0.27 and 0.29. Clearly, the main components of PSR J2323+1214 cannot be fitted with a Weibull distribution despite the large range of k being searched ($0 < k < 10$). The secondary component still agrees with a Weibull distribution, note that its *runs* test does show deviation from a Poisson toward over-clustering.

PSR J0539+0013’s waiting times are still consistent with a Weibull distribution. The statistical analysis of the waiting time helps establish stronger evidence that the pulses are truly emitted intermittently rather than simply varying in brightness. Furthermore, our K-S test rejected the Weibull distribution with a range of k values, which means that the single pulse waiting times probably cannot be explained by an over-clustered Poisson process. With future longer observations, the waiting time analysis may help us test more scenarios of pulsar emission physics than what the simple *runs* test can do.

Nulling Period Analysis: Since the first periodic nulling system was discovered (Herfindal & Rankin 2007), more such behavior has been identified in slow pulsars (Herfindal & Rankin 2007; Rankin & Wright 2008; Herfindal & Rankin 2009; Basu et al. 2017; Basu & Mitra 2018, 2019; Basu et al. 2020b). We relied on the periodogram-based method in PSRSALAS to search

for potential periodicity in the single pulses of the two slow pulsars. We found no detections of a period in the two components of PSR J2323+1214 and we found a marginal detection (4.4σ level) of a sub-pulse-drift or recurrent period of 32.3 ± 0.4 rotations (Fig. 10) from PSR J0539+0013.

3 RESULTS

PSR J2323+1214 is a slow pulsar with a period of 3759.5 ms and a DM of 26.7 pc cm^{-3} (Table 2). Cameron et al. (2020) timed this pulsar using the Parkes telescope and obtained its precise P and \dot{P} values. They show that this pulsar has a rotational energy loss rate of $\dot{E} = 1.37 \times 10^{30} \text{ erg s}^{-1}$. Due to its slow rotation, this pulsar is close to or beyond some of the theoretical “death lines” for pulsars (Ruderman & Sutherland 1975; Arons & Scharlemann 1979; Zhang et al. 2000; Harding et al. 2002). We present the single pulse study of this pulsar in Section 2.3. The pulsar’s secondary component seems to be nulling more often than its main component. We found a nulling fraction of $(80 \pm 2)\%$ for its main component and $(87 \pm 1)\%$ for its secondary component (Fig. 4).

We test the waiting time distribution of PSR J2323+1214’s main pulse with a Weibull distribution but could not find any acceptable fit with a range of shape parameter values ($0 < k < 10$). The rejection of a Weibull distribution favors the idea that the pulses are emitted in a non-Poisson bursting process. We also search for sub-pulse-drift or recurrent period in the single pulses of the two components of PSR J2323+1214 in their periodogram by using PSRSALAS and find no evidence of any period, possibly due to the limited length of the observation (Fig. 6).

PSR J0539+0013 has a period of 4710.2 ms and a DM of 49.0 pc cm^{-3} (Table 2). The pulsar has two components with a bridge emission linking the two (Fig. 8). It exhibits pulse-to-pulse variations and a nulling fraction of $(84 \pm 2)\%$. The single pulse waiting time histogram is consistent with the Weibull distribution (Fig. 9). Utilizing a periodogram-based method in PSRSALAS, we find marginal detection (4.4σ level) of a sub-pulse-drift or recurrent period of 32.3 ± 0.4 rotations (Fig. 10). This makes PSR J0539+0013 an addition to the 29 known periodic nulling pulsars (Basu et al. 2020b). It is noted that periodic nulling and amplitude modulations may be related to periodic modulation in the pulse profile or subpulse drifting, but this is clearly not the case for at least some pulsars (Basu et al. 2020b). For example, Basu et al. (2020a) observe PSR B2000+40 (PSR J2002+4050) at 1.6 GHz employing the Effelsberg and find a shorter prominent period ($2.5P$) associated with the subpulse

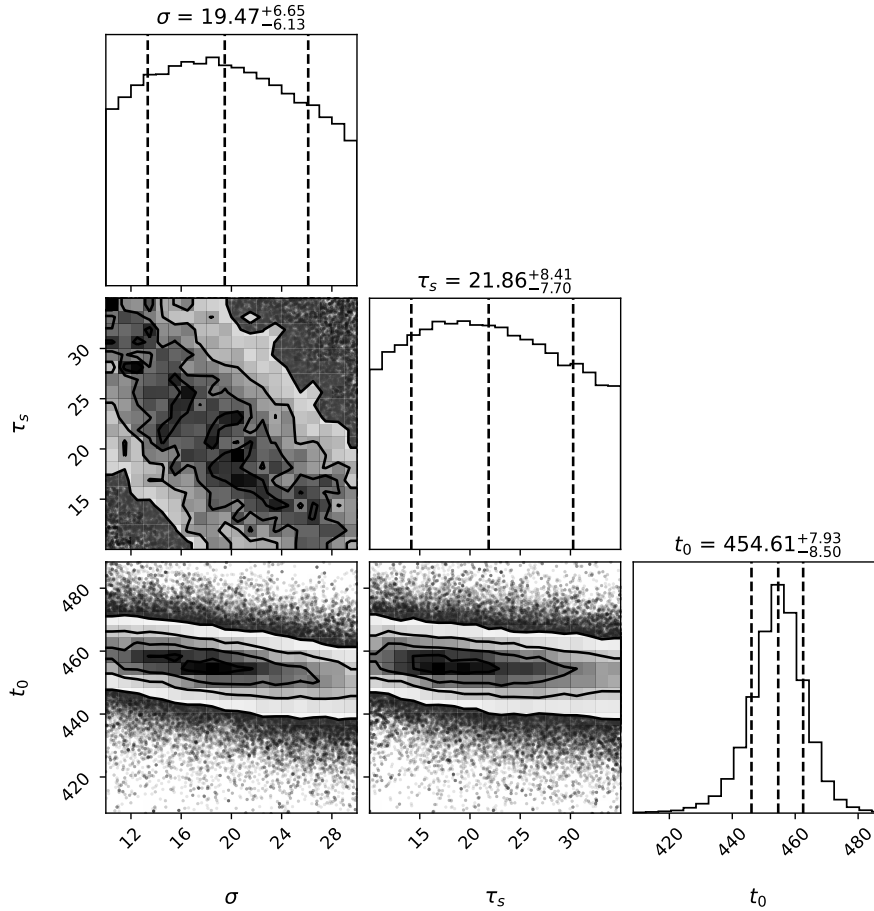


Fig. 12 Posterior distributions of σ , τ_s (centered at 327 MHz) and t_0 (the pulse arrival time relative to the starting point) obtained by using *emcee*. The dashed lines represent 16, 50 and 84 percentiles in the corresponding histograms.

drifting phenomenon and a longer period ($40P$) associated with nulling behavior. Interestingly, PSR J0539+0013’s waiting times are also shorter than the tentative recurrent period of 32.3 ± 0.4 rotations. In the canonical view of pulsar polar-cap radiation (Ruderman & Sutherland 1975), there may be two distinct mechanisms at work in these nulling pulsars. One sparking mechanism that causes the short-term nulls and operates at a shorter timescale from a few to ten rotations, and one periodic driving mechanism (possibly related to profile modulation or sub-pulse drifting) that operates at a longer timescale from tens to hundreds of rotations. The Arecibo observations presented in this work pave the way for longer and more detailed single pulse behavior studies of these slow pulsars that could be helpful for understanding the link between nulling and pulse modulation.

PSR J0539+0013’s periodogram analysis manifests a recurring period and its waiting time follows a Weibull distribution with $k \sim 1$. On the contrary, PSR J2323+1214’s waiting time clearly deviates from a

Poisson process, but its pulses display no recurring period. The contrast between the two slow pulsars may be the result of the limited lengths of our observations. In future longer observations, we may constrain their behavior to a better degree and find interesting new patterns from them.

PSR J1844+2135 has a period of 594.7 ms and a DM of 29.1 pc cm^{-3} (Table 2) and has a scattering tail in its pulse profile. We model its pulse profile in Figure 11 as a Gaussian pulse profile convolved with a one-sided exponential scattering tail. Utilizing *emcee* (Foreman-Mackey et al. 2013), we obtain the best-fit value of the pulse width (σ) and the scattering timescale (τ_s) at 327 MHz as featured in Figure 12.

PSR J2057+2133 has a period of 1166.7 ms and a DM of 72.2 pc cm^{-3} (Table 2). PSR J2057+2133 is far away from the Scutum-Crux Arm. As illustrated in Figure 1, there are very few pulsars around PSR J2057+2133, which means the Galactic free electron density model of this area is probably not accurate. This pulsar could potentially be

used to update the electron density model of this direction if its distance is measured precisely in the future.

PSR J0209+2621 has a period of 1934.8 ms and a DM of 23.7 pc cm^{-3} (Table 2). PSR J2111+2132 has a DM of 78.5 pc cm^{-3} , larger than the upper limits in this direction from two Galactic free electron density models (Table 2: NE2001 is 77.7 pc cm^{-3} , YMW16 is 63.6 pc cm^{-3}). PSR J2025+2133 is near PSR J2111+2132, thus it was discovered and confirmed the same day by FAST and Arecibo. It has a period of 623.5 ms and a DM of 70.8 pc cm^{-3} (Table 2).

CRAFTS is a shallow, but unbiased survey. A steady stream of new pulsars is being discovered. Further study of these sources, constraining their distances, in particular, will help refine the Galactic free electron density model. The slow-pulsar single-pulse behaviors presented in the study, along with the upcoming CRAFTS samples, could add to the samples of sub-pulse-drifting and nulling/bursting pulsars and help understand the pulsar radio wave emission mechanisms in the future.

4 CONCLUSIONS

We present Arecibo confirmation and follow-up studies of seven FAST pulsars discovered in the CRAFTS-UWB survey and better-quality single pulse studies of two slow extreme nulling pulsars. Our main findings are:

(1) PSR J0209+2621, PSR J1844+2135, PSR J2111+2132, PSR J2025+2133 and PSR J2057+2133 are normal pulsars with periods between 0.59 s and 1.93 s. PSR J2323+1214 and PSR J0539+0013 are slow extreme nulling pulsars with periods 3.76 s and 4.71 s, respectively.

(2) All seven pulsars have DMs lower than 80 pc cm^{-3} . PSR J2111+2132's DM is larger than the upper limit of the Galactic free electron density models. PSR J2057+2133 is away from the Scutum-Crux Arm. Its expected distance from the YMW16 model is 3 times that of the NE2001 model, reflecting the relatively large uncertainties for the electron densities in the local volume. More discoveries like this one will help improve the Galactic electron density model in the future.

(3) PSR J2323+1214 is a slow pulsar with two components. It has a nulling fraction of $(80 \pm 2)\%$ for its main component and $(87 \pm 1)\%$ for its secondary component. We find no sub-pulse-drift or recurrent period for its main or secondary components. We conclude that this pulsar seems to emit pulses in bursts of two to three counts then nulls for several rotations. Its main component's pulse waiting time distribution cannot be fitted with a Poisson-like distribution, favoring a non-uniform emission triggering mechanism.

(4) PSR J0539+0013 is a nulling slow pulsar with two components and nulling fraction of $(84 \pm 2)\%$. It has a drift or recurrent period of about 32.3 ± 0.4 . The single pulses of this pulsar seem to come in bursts of two to three pulses while the burst waiting time distribution could still be fitted with a Weibull distribution. Thus, we cannot rule out the pulses being from a Poisson-like process.

(5) PSR J1844+2132 has a clear scattering tail with a scattering timescale of $\tau_s = 22 \pm 8$ ms.

Acknowledgements We thank the referee for the constructive review. This work is supported by the National Natural Science Foundation of China (Grant Nos. 11988101, U2031117, 11725313, 12041303, 11873067, U1831131 and U1631132), the China Scholarship Council (No. 201704910686), the CAS-MPG LEGACY project, the Strategic Priority Research Program of the Chinese Academy of Sciences (Grant No. XDB23000000) and the National SKA Program of China (No. 2020SKA0120200), the Foundation of Guizhou Provincial Education Department (No. KY(2020)003), the Cultivation Project for FAST Scientific Payoff and the Research Achievement of CAMS-CAS. We acknowledge Prof. Renxin Xu, Prof. Hongguang Wang and Dr. Jiguang Lu for their valuable discussions. We acknowledge the group of the FAST telescope. We are particularly grateful to the group associated with the Arecibo telescope. Before Arecibo was damaged, we confirmed tens of FAST pulsars with the support of Arecibo groups, especially these special pulsars presented here. Arecibo offers its shoulders of giants to help FAST see further and better!

References

- Arons, J., & Scharlemann, E. T. 1979, *ApJ*, 231, 854
 Backer, D. C. 1970, *Nature*, 228, 1297
 Basu, R., Lewandowski, W., & Kijak, J. 2020a, *MNRAS*, 499, 906
 Basu, R., & Mitra, D. 2018, *MNRAS*, 476, 1345
 Basu, R., & Mitra, D. 2019, *MNRAS*, 487, 4536
 Basu, R., Mitra, D., & Melikidze, G. I. 2017, *ApJ*, 846, 109
 Basu, R., Mitra, D., & Melikidze, G. I. 2020b, *ApJ*, 889, 133
 Biggs, J. D. 1992, *ApJ*, 394, 574
 Cameron, A. D., Li, D., Hobbs, G., et al. 2020, *MNRAS*, 495, 3515
 Cordes, J. M. 2013, *ApJ*, 775, 47
 Filippenko, A. V., & Radhakrishnan, V. 1982, *ApJ*, 263, 828
 Foreman-Mackey, D., Hogg, D. W., Lang, D., & Goodman, J. 2013, *PASP*, 125, 306
 Gajjar, V., Joshi, B. C., & Kramer, M. 2012, *MNRAS*, 424, 1197
 Gajjar, V., Joshi, B. C., & Wright, G. 2014, *MNRAS*, 439, 221
 Gil, J., Melikidze, G. I., & Geppert, U. 2003, *A&A*, 407, 315
 Han, J. L., Wang, C., Wang, P. F., et al. 2021, *RAA (Research in Astronomy and Astrophysics)*, 21, 107

- Harding, A. K., Strickman, M. S., Gwinn, C., et al. 2002, *ApJ*, 576, 376
- Herfindal, J. L., & Rankin, J. M. 2007, *MNRAS*, 380, 430
- Herfindal, J. L., & Rankin, J. M. 2009, *MNRAS*, 393, 1391
- Hewish, A., Bell, S. J., Pilkington, J. D. H., Scott, P. F., & Collins, R. A. 1968, *Nature*, 217, 709
- Hotan, A. W., van Straten, W., & Manchester, R. N. 2004, *PASA*, 21, 302
- Jiang, P., Yue, Y., Gan, H., et al. 2019, *Science China Physics, Mechanics, and Astronomy*, 62, 959502
- Konar, S., & Deka, U. 2019, *Journal of Astrophysics and Astronomy*, 40, 42
- Li, D., Dickey, J. M., & Liu, S. 2019, *RAA (Research in Astronomy and Astrophysics)*, 19, 016
- Li, D., Wang, P., Qian, L., et al. 2018, *IEEE Microwave Magazine*, 19, 112
- Lorimer, D. R., Faulkner, A. J., Lyne, A. G., et al. 2006, *MNRAS*, 372, 777
- Lyne, A., Hobbs, G., Kramer, M., Stairs, I., & Stappers, B. 2010, *Science*, 329, 408
- Naidu, A., Joshi, B. C., Manoharan, P. K., & Krishnakumar, M. A. 2018, *MNRAS*, 475, 2375
- Nan, R., Li, D., Jin, C., et al. 2011, *International Journal of Modern Physics D*, 20, 989
- Oppermann, N., Yu, H.-R., & Pen, U.-L. 2018, *MNRAS*, 475, 5109
- Qian, L., Pan, Z., Li, D., et al. 2019, *Science China Physics, Mechanics, and Astronomy*, 62, 959508
- Rankin, J. M., & Wright, G. A. E. 2008, *MNRAS*, 385, 1923
- Redman, S. L., & Rankin, J. M. 2009, *MNRAS*, 395, 1529
- Ritchings, R. T. 1976, *MNRAS*, 176, 249
- Ruderman, M. A., & Sutherland, P. G. 1975, *ApJ*, 196, 51
- Sheikh, S. Z., & MacDonald, M. G. 2021, *MNRAS*, 502, 4669
- Szary, A., Melikidze, G. I., & Gil, J. 2015, *MNRAS*, 447, 2295
- van Straten, W., & Bailes, M. 2010, *DSPSR: Digital Signal Processing Software for Pulsar Astronomy*
- Wald, A., & Wolfowitz, J. 1940, *The Annals of Mathematical Statistics*, 11, 147
- Wang, N., Manchester, R. N., & Johnston, S. 2007, *MNRAS*, 377, 1383
- Weltevrede, P. 2016, *A&A*, 590, A109
- Weltevrede, P., Wright, G. A. E., Stappers, B. W., & Rankin, J. M. 2006, *A&A*, 458, 269
- Yu, Q.-Y., Pan, Z.-C., Qian, L., et al. 2020, *RAA (Research in Astronomy and Astrophysics)*, 20, 091
- Zhang, B., Harding, A. K., & Muslimov, A. G. 2000, *ApJL*, 531, L135
- Zhu, W. W., Berndsen, A., Madsen, E. C., et al. 2014, *ApJ*, 781, 117